Docking Model of Drug Binding to the Human Ether-à-go-go Potassium Channel Guided by Tandem Dimer Mutant Patch-Clamp Data: A Synergic Approach

Yumi N. Imai,[†] Sunghi Ryu,[†] and Shigetoshi Oiki*[,‡]

Discovery Research Center, Pharmaceutical Research Division, Takeda Pharmaceutical Company Ltd., Osaka 532-8686, Japan, and Department of Molecular Physiology and Biophysics, Faculty of Medical Sciences, University of Fukui, Fukui 910-1193, Japan

Received September 30, 2008

To characterize drug binding to the human ether-à-go-go related gene (hERG) channel, a synergic approach interplaying patch-clamp experiments and a docking study was developed. Mutations were introduced into concatenated dimers of the hERG channel that were assembled into a heterotetramer with mutated diagonal subunits. The binding affinities of three drugs (cisapride, terfenadine, and *N*-[4-[[1-[2-(6-methyl-2-pyridinyl)ethyl]-4-piperidinyl]carbonyl]phenyl]methanesulfonamide dihydrochloride (E-4031, **1**)) to a set of mutant channels were examined electrophysiologically to assess the involved residues, their number, and relative positions. Cisapride and **1** interacted with Tyr652 residues on adjacent subunits, while terfenadine interacted with Tyr652 residues on diagonal, but not on adjacent, subunits. Phe656 was involved in the binding of all three drugs, and Ser624 was found to be only involved in cisapride and **1**. The docking models demonstrated that $\pi-\pi$ and CH$-\pi$ interactions rather than cation$-\pi$ interaction play a key role in drug binding to the hERG channel.

Introduction

Long QT syndrome (LQTS[a]) is a disorder of ventricular repolarization that predisposes affected individuals to be afflicted with cardiac arrhythmias and sudden death. A cardiac potassium channel, the human ether-à-go-go related gene (hERG) channel, has been linked to prolongation of the QT interval in electrocardiograms (ECG), and mutations in the hERG gene are the cause of inherited LQTS.[1] LQTS may also be of an acquired type, in which various medications exert a blocking effect on hERG channels.[2] The list of drugs that block hERG channels is growing, and they encompass a rich repertoire of chemotypes and therapeutic classes, suggesting that no single pharmacophore may be responsible for hERG blockade. The broad diversity of the blocking drugs has complicated efforts to elucidate the mechanism of these drug−channel interactions.

To eliminate hERG side effects by structure-based drug design, characterization of the drug binding site and binding modes is necessary. From electrophysiological studies, it has been revealed that many hERG blockers bind to the channel when the activation gate is open,[3] thus indicating that the binding site is located in the structural passage of the pore. For potassium channels, functional channels are assembled as homotetramers and the sixth transmembrane helices line the pore. Mutations of aromatic residues (Tyr652 and Phe656) on the sixth transmembrane helix dramatically attenuate the binding affinity of typical hERG blockers, such as cisapride, terfenadine, and *N*-[1′-(6-cyano-1,2,3,4-tetrahydronaphthalen-2-yl)-4-hydroxyspiro[3,4-dihydrochromene-2,4′-piperidine]-6-yl]methanesulfonamide (MK-499).[4−6] Furthermore, a contribution to the binding process by Ser624, which is located at the C-terminal end of the pore helix, has been suggested.[7] It is likely that these residues are clustered to form the binding site in the three-dimensional structure of a hERG channel. In these studies, the mutations were introduced into the monomeric subunits, which are assembled into the homotetrameric channel and have mutated sites in the four symmetrical positions. On the other hand, hERG-blocking drugs have an asymmetrical structure with a molecular size sufficiently large to span multiple subunits. In this respect, the earlier mutational studies, except for ours,[8] were designed to identify the residues involved in binding, and the specification of the number and positions of the involved residues has been left unanswered for the time being.

Here, we propose a synergic approach for elucidating the binding mode of drugs to the hERG channel. In this study, we focused on Tyr652, Phe656, and Ser624 for the mutational sites, since Tyr652 and Phe656 are considered key aromatic residues for the π-related or hydrophobic interactions[7,9] and since Ser624 is placed at the entrance of the selectivity filter, where various types of drugs can form hydrogen bonds and effectively intercept the potassium permeation.[7] A tandem dimer of the hERG channel was constructed, and a mutation was introduced into one of the subunits.[8,10] The mutant tandem dimers were readily assembled into functional channels with two mutated subunits on the diagonal positions. Six different channels, including tandem dimeric and homotetrameric mutants, were examined electrophysiologically for drug−inhibition curves and thus their drug binding affinities. We found that the set of drug−inhibition curves for each drug showed typical patterns of the curve shift for the tandem dimer, relative to those of wild type (WT) and the homotetrameric mutant. The patterns of the drug inhibition curves helped identify the number and position of the contributing residues, and incorporating the binding information into docking studies allowed the prediction of plausible binding modes for the drugs. We applied this approach to the well-established hERG blockers, cisapride, terfenadine, and *N*-[4-[[1-[2-(6-methyl-2-pyridinyl)ethyl]-4-piperidinyl]carbonyl]phenyl]methanesulfonamide dihydrochloride (E-4031, **1**),[11] and the characteristics of the interactions between the drugs and specific

* To whom correspondence should be addressed. Telephone: +81-776-61-8306. Fax: +81-776-61-8101. E-mail: oiki-fki@umin.ac.jp.

† Takeda Pharmaceutical Company Ltd.

‡ University of Fukui.

[a] Abbreviation: hERG, human ether-à-go-go related gene; LQTS, long QT syndrome; ECG, electrocardiograms; WT, wild type; HEK-293, human embryonic kidney (cells); PCR, polymerase chain reaction; MEM, minimum Eagle medium; $I_{drug}/I_{control}$, normalized current amplitude; DMSO, dimethyl sulfoxide.

10.1021/jm801236n CCC: $40.75
Published on Web 03/05/2009

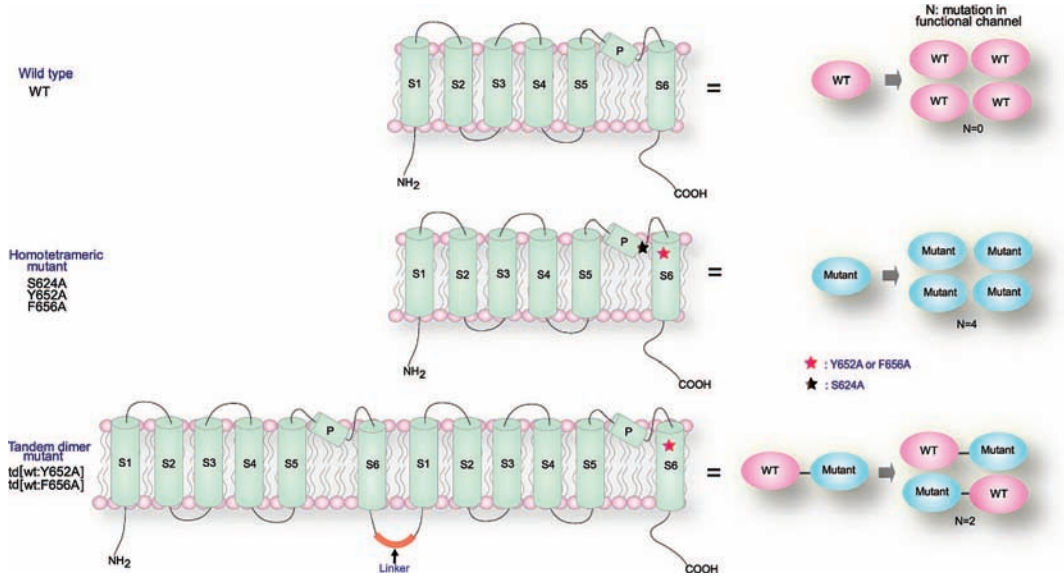

Figure 1. Manipulating the numbers of mutated subunits and their relative positions in the functional tetrameric channels. Each subunit is composed of six transmembrane helices, with the sixth transmembrane helices lining the pore. In the right column, depictions of channel assembly are shown in which the WT subunits are indicated by pink circles and the mutated subunits by blue circles. Tandem dimers are shown as a concatenated molecule of the WT and mutant subunits with a short linker.

residues of the hERG channel are discussed. This information will be exploited in practical drug discovery projects to develop drugs with fewer or no side effects to their hERG channel activity.

Results and Discussion

Expression of Mutant Channels and Patch-Clamp Recordings. We constructed a tandem dimer with a short linker, and a point mutation was introduced into one of the subunits (see Experimental Section). When functional channels were assembled, mutational sites should be located on subunits in the diagonal position of the tetrameric channel (Figure 1). Mutants in the monomeric sequence were also produced, and these were assembled into homotetrameric channels having four mutational sites in symmetrical positions. In this study Tyr652, Phe656, and Ser624 were mutated to alanine and six types of channels (WT, homotetrameric mutants (Y652A, F656A, and S624A), and tandem dimer mutants (td[wt:Y652A], td[wt:F656A]) were examined.

Tandem dimer mutants or monomer mutants were stably expressed in human embryonic kidney (HEK-293) cells. Whole-cell patch clamp recordings were performed at room temperature, and potassium currents were elicited by depolarization pulses (Figure 2A). Similar but slightly modified current traces, compared to those for WT, were attained from a tandem dimer without mutation (td[wt:wt]), indicating concatenation had not affected the expression and gating of the channel (not shown).[9] Extracellular solutions were continually perfused throughout the recordings, and the peak amplitudes of the tail current at −40 or −120 mV were measured at different concentrations of drugs.

Patterns of Drug−Inhibition Curves for the Mutant Channels. In the presence of cisapride, current amplitudes at the depolarization and repolarization pulses were depressed significantly for WT and a tandem dimer mutant (td[wt:Y652A]) but not for a homotetrameric mutant (Y652A) (Figure 2A, upper traces). Normalized current amplitudes ($I_{drug}/I_{control}$) were plotted as a function of drug concentrations (Figure 2B), and the data were fitted with the inhibition curve. The binding affinity of Y652A mutant was more than 50 times lower than that for WT, confirming that Tyr652 plays an essential role for the binding. The inhibition curve for td[wt:Y652A] was shifted to the right significantly compared with that of WT (part a of Figure 2B). Shift would never occur if the drug interacted with a residue from a single subunit or at most two residues from diagonal subunits, since relevant residue(s) are retained in the tandem dimer mutants. Therefore, the right shift or the lower affinity for td[wt:Y652A] indicates that Y652 groups on adjacent subunits contribute to the binding. In contrast to Tyr652, the current traces (Figure 2A, lower traces) and the inhibition curves for WT and td[wt:F656A] were indistinguishable, even though the homotetrameric mutant F656A displays an affinity that is 170 times lower. These results indicate that the Phe656s on the two adjacent subunits do not contribute to the binding, but rather one or two of the Phe656s on the diagonal subunits participate in the binding.

The above logical program was formalized as a simple procedure involving pattern recognition. We present here a visual inspection method for identifying the number and relative position of residues contributing to the binding. For each type of residue relevant to drug binding, inhibition curves were drawn for a homotetrameric mutant channel and the tandem dimeric mutant channel, as well as for WT (Figure 2B). Among three inhibition curves, the relative position of the curve for the tandem dimer is crucial. If a drug interacts with the type of residue from one subunit, or at most two of the diagonal subunits, then the inhibition curve of the tandem dimer should overlap with that of WT. In contrast, if two residues from adjacent subunits contribute to the binding, the inhibition curve for the tandem dimer channel should be located between those of the WT and homotetrameric mutant channels. Thus, by simple inspection of the inhibition curve for the tandem dimer, the contribution made by residues from either a single (or diagonal) or adjacent subunits can be evaluated.

Parts c and d of Figure 2B shows results for **1**, which is similar to that for cisapride. On the other hand, for terfenadine the inhibition curves for the tandem dimer were indistinguishable from those of WT (parts e and f Figure 2B), demonstrating that only Tyr652 and Phe656 on the diagonal subunits contribute to the drug binding.

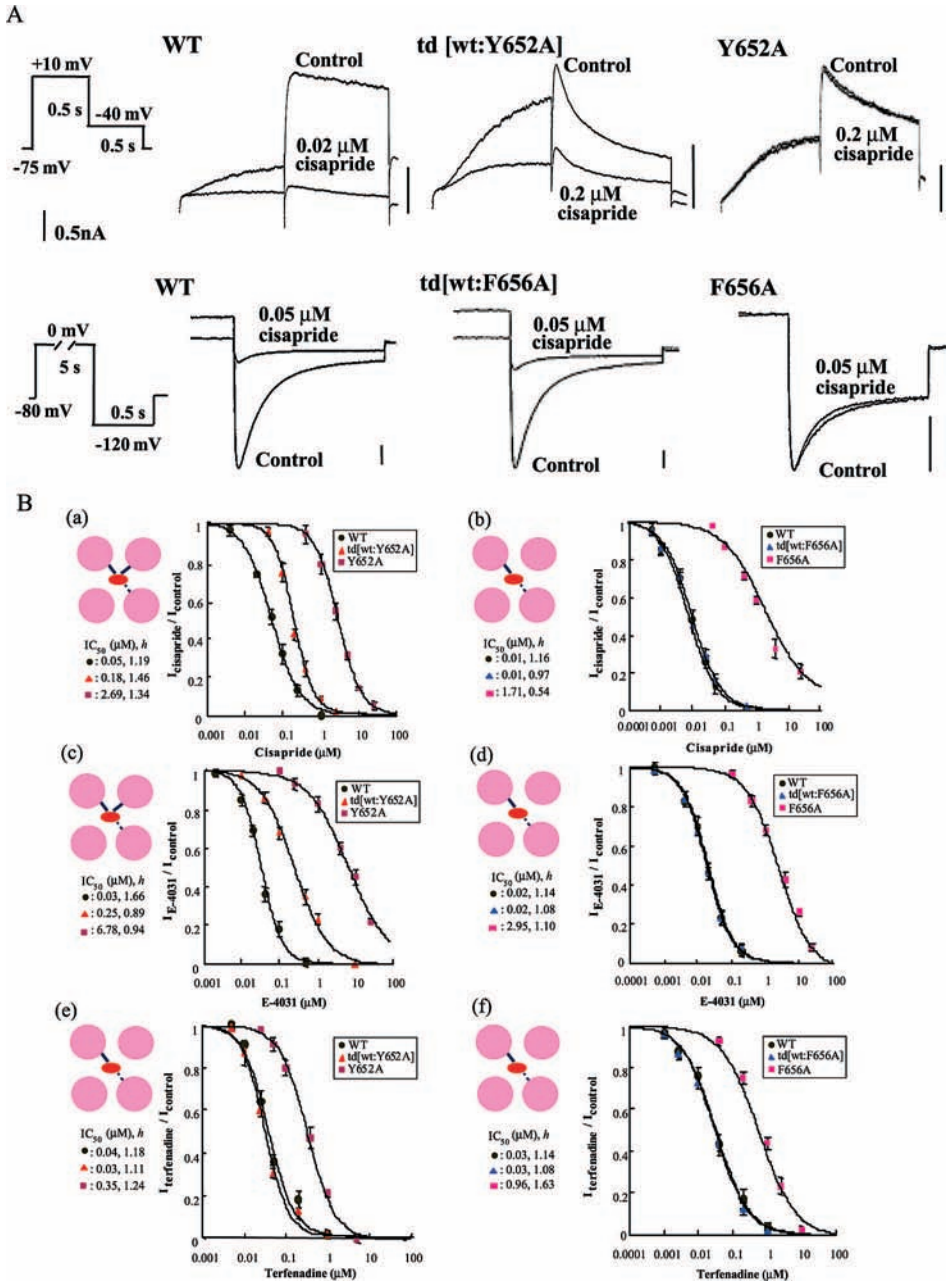

Figure 2. Blocking of hERG currents by drugs. (A) Representative current traces of WT and the mutants at cisapride concentrations of 0.02 μM (Y652 mutations) and 0.05 μM (F656 mutations). Note that the concentration of cisapride was 10 times lower for WT than that for td[wt:Y652A] but the degree of the blocking of WT and td[wt:Y652A] was similar. (B) Drug inhibition curves for cisapride (a, b), **1** (c, d), and terfenadine (e, f). In each panel, the three inhibition curves are for WT, the tandem dimer mutant, and the homotetrameric mutant. The left column of the panels shows the Y652 mutations, and the right shows the F656 mutations. The schematic illustrations represent the possible contribution of residues to the binding on the subunits. Red oval disks represent drugs interacting with residues on the subunits (thick lines indicate positive interactions, and broken lines indicate possible interactions). Data were fitted with the Hill equation yielding an IC_{50} and a Hill coefficient (h) (mean values are shown in figure).

The contributions of Ser624 were also examined electrophysiologically. The affinity of drugs for the S624A mutant was significantly reduced for cisapride and **1**, whereas it was almost identical for terfenadine (Figure 3). These observations suggest that Ser624 is involved in the blockade of cisapride and **1** but not terfenadine.[12]

On the basis of the topological information of the binding from the electrophysiological results, followed by the pattern recognition found in the drug inhibition curves, docking studies were performed for the three compounds.

Modeling the Binding Site of the hERG Channel for Docking Studies. The pore domain, the S5−pore−S6 helices of the hERG channel, was constructed by homology modeling based on the sequence alignment (Figure 4) and the crystal structures of potassium channels in closed (KcsA, PDB code 1BL8) and open (MthK, PDB code 1LNQ; KvAP, PDB code 1ORQ) states as templates. To be consistent with the above experimental results, the following criteria were used for selecting the model. First, Tyr652, Phe656, and Ser624 should be exposed to the surface of the drug-binding region. Second,

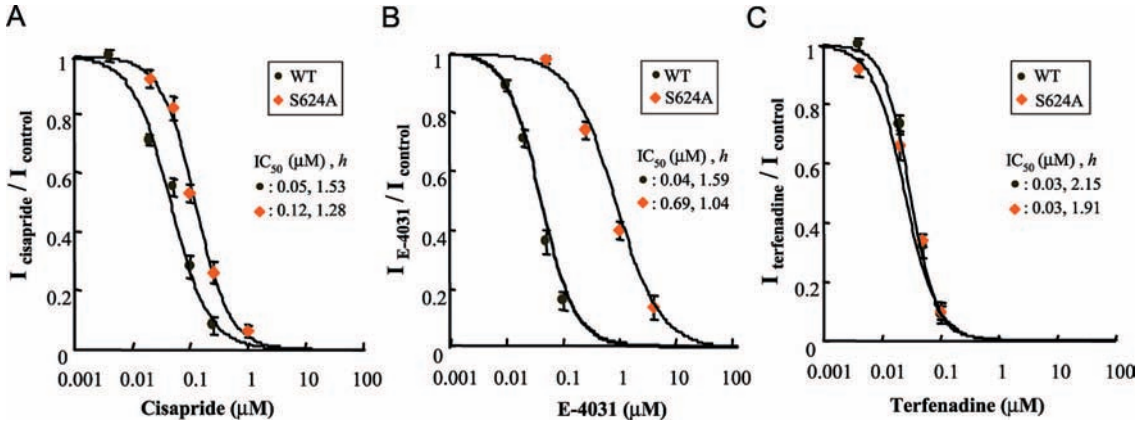

Figure 3. Concentration-dependent blockades of WT and S624A hERG channels by cisapride (A), **1** (B), and terfenadine (C). Data were fitted with the Hill equation yielding an IC_{50} and a Hill coefficient (*h*) (mean values are shown in figure).

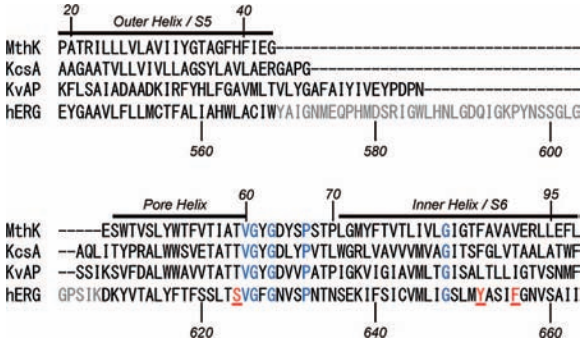

Figure 4. Sequence alignment of the S5−pore−S6 helices region for the MthK, KcsA, KvAP channels and the equivalent residues from the S5 to S6 transmembrane domains of the hERG channel. The sequences of the MthK (upper) and hERG (lower) channels are numbered. The identical residues among four channels are colored blue, and the residues in the loop region of the hERG channel omitted from the present model are colored gray. The residues of hERG channel mutated with Ala in this work are colored red and underlined.

the distances between aromatic residues on the adjacent subunits and diagonal subunits for the model channels were gauged by whether the drugs could interact with respective residues on the models in a way compatible with the experimental results.

The KcsA derived closed state model allowed all Tyr652, Phe656, and Ser624 side chains in all subunits to be simultaneously exposed to the surface. However, the distance between Phe656 residues was extremely close (3.3 Å for adjacent subunits and 4.9 Å for diagonal subunits). The diameter of the pore at the Phe656 level was so narrow that an aromatic ring of drugs, once placed at this level, would be surrounded by Phe656 groups and have contact with all of them simultaneously. On the other hand, at the Tyr652 level, the pore cavity became ample where drugs had been sequestered and interaction with Phe656 was unavoidable. These modes of interaction are not compatible with the experimental results that a drug may interact with either two adjacent subunits or a single one.

The KvAP derived open state model demonstrated shielding of the Tyr652 side chain behind Phe656 such that drugs cannot gain access to the Tyr652, failing the criteria for the binding site. To circumvent the issue, Farid et al. applied the "induced-fit" docking methodology, in which flexible parts of the backbone were modified to expose Tyr652 to the surface of the pore region.[13] However, the predicted binding modes for cisapride and terfenadine (three Tyr652 residues and two adjacent Phe656 residues are simultaneously involved in the interaction with cisapride, and four Tyr652 residues and two diagonal Phe656 residues with terfenadine) were quite different from our experimental results.

The initial structure of the MthK derived open state model showed the Tyr652 and Phe656 residues exposed to the surface, but Ser624 could not contribute to the drug binding. Therefore, the structure of the selectivity filter was slightly relaxed within the range of 7 Å from the Ser624 residues by molecular mechanics. The main chain structure in the selectivity filter region became somewhat collapsed from the template, and Ser624 and Thr623 then became readily accessed by drugs, which may explain the results of the mutational studies. In this procedure Tyr652 and Phr656 were almost unaltered and stayed exposed to the surface. It has been established that many drugs exhibit a stronger affinity to the inactivated or partially collapsed filter structure rather than to the open or open-filter structure.[14,15] In this respect, our procedure for the model refinement may correspond to structural transitions to the "inactivated" state. The MthK derived model used in the docking studies is shown in Figure 5A,B and Supporting Information. We found in this model that Thr623 was in proximity to Tyr652 and thus ready for hydrogen bonding, as shown in Figure 5C. Similar close packing in open form was predicted from the KvAP derived model by Farid et al.[13]

Proposed Binding Modes for Cisapride, 1, and Terfenadine. Binding poses of drugs (cisapride, **1**, and terfenadine) in the hERG pore region were generated extensively using the program Gold, followed by selection with the subsequent criteria. First, all binding modes satisfying the number and relative positions of the residues involved for the drug binding were selected by visual inspection. Second, the π-related interactions of the aromatic rings in Tyr652 and Phe656 were a particular focus, since those interaction energies, such as CH$-\pi$ and $\pi-\pi$ interactions, were reported to be -1.454 kcal/mol for CH$-\pi$ interactions[16] and -1.81 to -2.78 kcal/mol for $\pi-\pi$ interactions[17] by ab initio quantum chemistry methods, which stabilize the binding notably. In the selection procedure for the optimal configurations, however, the ranking of the docking configurations by the scores was inadequate, since the docking programs do not implement the docking parameters for the π-related interactions. Thus, configurations were selected on the basis of drug contacts with Tyr652 and/or Phe656, and the distance between atoms or centroids of an aromatic ring in a drug molecule and a side chain should be within 4.5 Å. This distance criterion is based on the crystal structure of the tetrabutylammonium (TBA)-bound KcsA channel (PDB code 1J95), in which the distance between the ethyl group of TBA and adjacent residues was 4.5 Å.[18] Third, the experimental

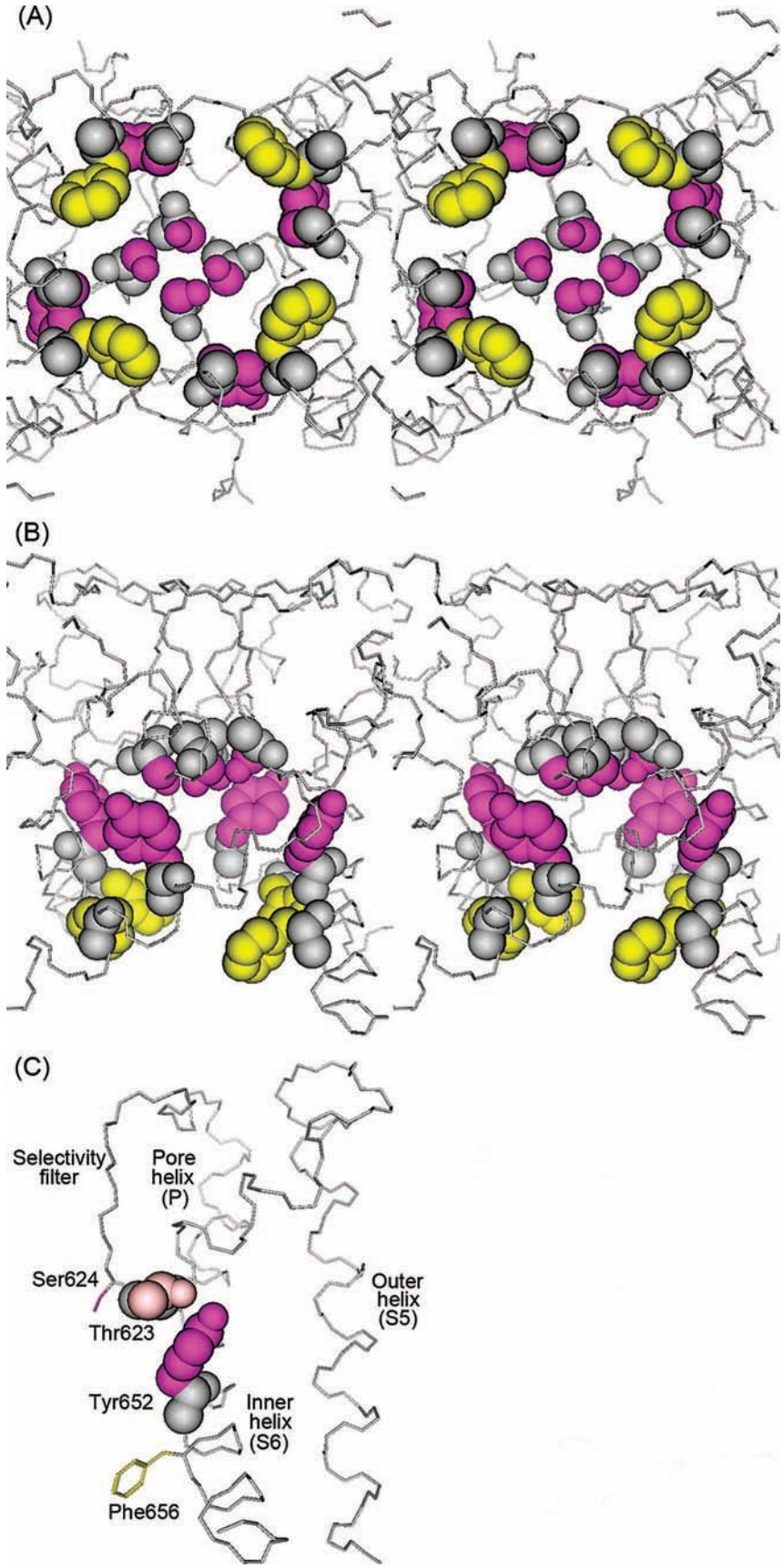

Figure 5. MthK derived homology model (open form) used in the docking studies. (A) The stereodrawing of the structure is viewed parallel to the central pore axis, from the intracellular side toward the selectivity filter. Ser624, Tyr652, and Phe656 are represented by the space-filling model. Side chains of Ser624 and Tyr652 are shown in magenta, and Phe656 is in yellow. (B) The stereodrawing of the structure is viewed from the side. Ser624, Tyr652, and Phe656 are represented by the space-filling model. Coloring is same as in (A). (C) Close packing between the side chains of Thr623 and Tyr652 predicted in the MthK derived open state model. The main chain structure of a subunit and only four residues are shown. Thr623 and Tyr652 are represented by a space-filling model, and Ser624 and Phe656 are represented by a stick model.

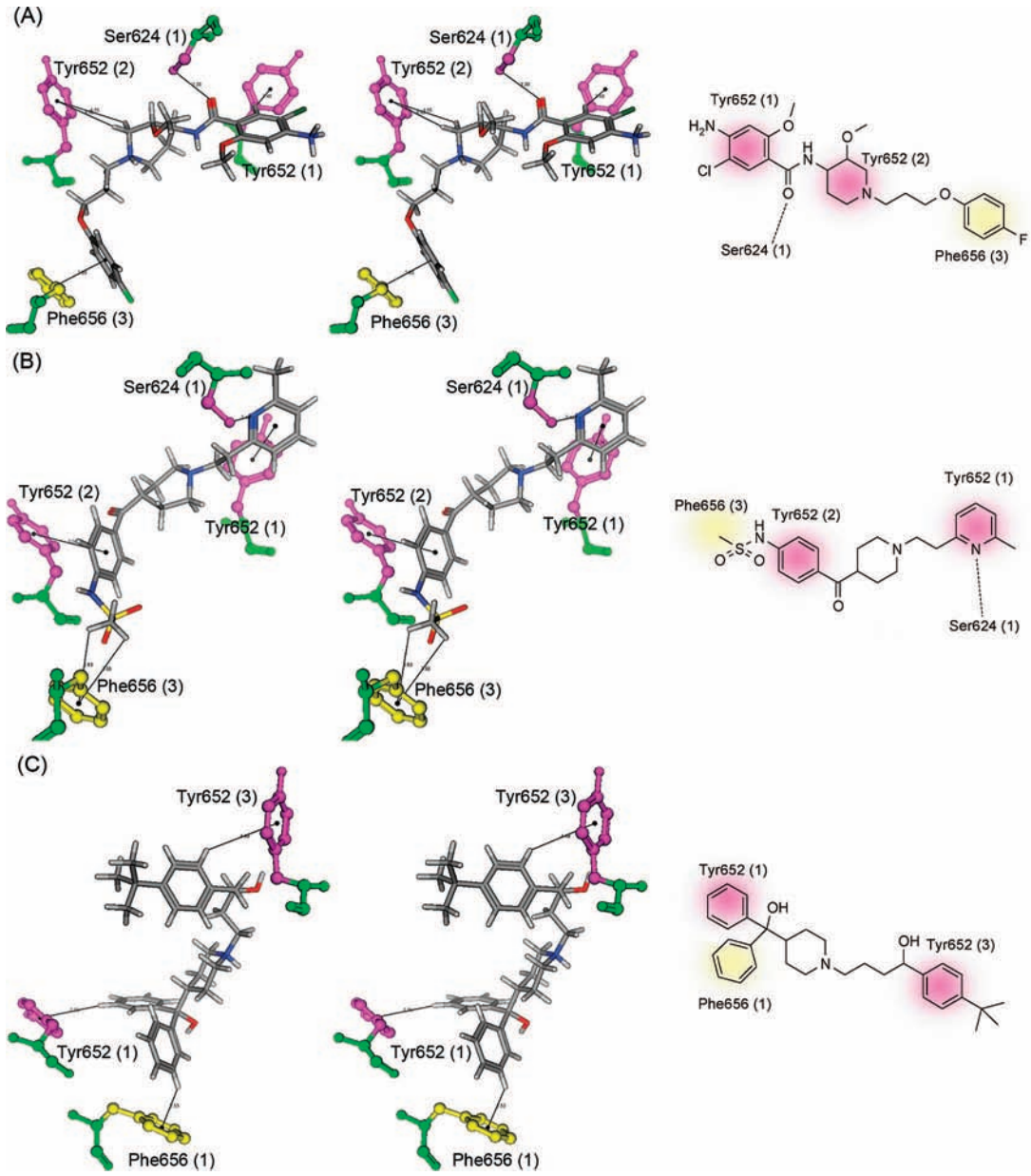

Figure 6. Proposed binding modes for cisapride (A), **1** (B), and terfenadine (C). Green represents the backbone atoms, yellow the hydrophobic side chains, magenta the polar side chains. The Ser624, Tyr652, and Phe656 residues that interact with blockers are represented by the ball and stick model. Compounds are drawn using wire models. The number in parentheses after the residue name represents the subunit number. The chemical structures with postulated binding mode are also shown in the right.

results on whether Ser624 contributes were incorporated for the purpose of selecting the binding configurations.

Figure 6A shows one of the binding modes for cisapride (Supporting Information), demonstrating that all three ring substructures were involved in the interaction. A Tyr652 side chain interacted with one of the terminal aromatic rings of cisapride via $\pi-\pi$ interaction (herringbone geometry), and the Tyr652 in the adjacent subunit interacted with the CH group adjacent to the cationic nitrogen in the central piperidine ring (CH$-\pi$ interaction). The latter is frequently observed in the crystal structures of protein−ligand complexes (For examples, PDB codes 1J17, 2BOH, 1O5M, 1QBO, etc), in which a CH group adjacent to a basic part, such as a piperidine nitrogen, comes close to an aromatic ring. In our model, the cationic nitrogen did not directly contribute to the binding. Another terminal aromatic ring was recognized by Phe656 in the third subunit via a $\pi-\pi$ interaction (stacked geometry), and the carbonyl oxygen of the amide group formed a hydrogen bond with Ser624.

Mosapride (see Chart 1), an analogue of cisapride possessing three ring substructures like cisapride, shows greatly reduced affinity to the hERG channel (IC_{50} = 4.8 μM),[19] even though both drugs possess potent agonistic activity to the serotonin 5-hydroxytryptamine 4 (5-HT(4)) receptor. To explore the attenuated interaction of mosapride to the hERG channel, mosapride was superimposed on the conformation of cisapride bound to the hERG binding site using the Flexible Alignment module in Molecular Operating Environment (MOE).[20] Figure 7 demonstrates that fluorophenyl group moieties of mosapride and cisapride did not overlap with each other. Since the interaction between the fluorophenyl group moieties of cisapride and Phe656 is important for cisapride binding, the change in the relative positions of the three rings induced by inserting a methylene group between the amide

Chart 1. Structures of the Compounds Found in This Work

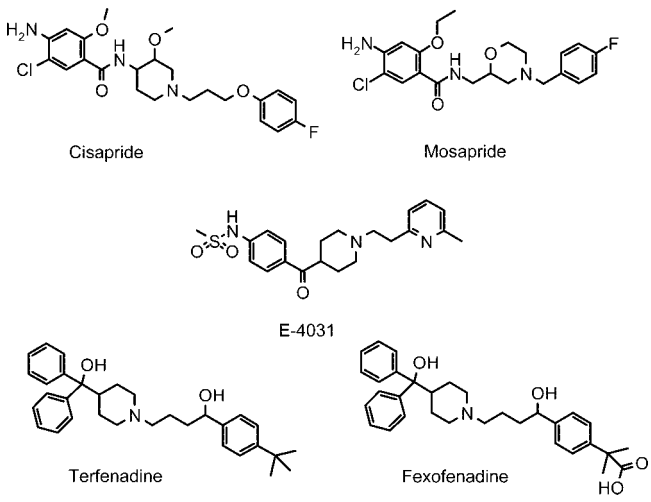

group and central ring system distinguishes mosapride from cisapride, which may lead to the elimination of hERG vulnerability.

For **1**, the experimental results demonstrated that the aromatic residues contributing to the binding were shared by cisapride. On the other hand, the inhibition pattern revealed that Ser624 contributed to **1** binding more dramatically than to cisapride (Figure 3A,B). Figure 6B shows one of the binding modes (Supporting Information), where Tyr652 ($\pi-\pi$ interaction, herringbone geometry) and Ser624 interacted with a terminal pyridine ring moiety. Phe656 was also involved in the CH$-\pi$ interaction with the methyl group in the methansulfonamide moiety. For **1** binding, the mutation of Thr623 was reported to attenuate the blocking, which has been modeled as formation of the hydrogen bond between Thr623 and the drug.[21] In our model, however, Thr623 was placed in proximity to Tyr652 to form hydrogen bonds, and we propose a hypothesis of Thr623 mutation to account for the experimental results. Thr623 likely stabilizes Tyr652 through hydrogen bonding, by which Tyr652 residues are faced toward the drug. Attenuated drug binding reported for the Thr623 mutation can be interpreted in our model that the replacement by alanine loses the hydrogen bond with Tyr652 and destabilizes the orientation of Tyr652, which is unfavorable for Tyr652−drug interactions.

For terfenadine binding, Figure 6C shows one of the binding modes obtained (Supporting Information), where two terminal aromatic rings interacted with the two diagonal Tyr652s, and another benzene ring of the benzhydryl group interacted with Phe656. All of the interactions in the binding of terfenadine to hERG are likely to be $\pi-\pi$ interactions (herringbone geometries). Farid et al. reported the postulated binding modes for terfenadine using an in silico method.[13] The involvement of four Tyr652s in the binding was inconsistent with our experimental results. On the basis of our binding mode, we present here a model example for modification of the terfenadine molecule to attenuate the binding (Figure 8): Introductions of electron withdrawing groups, such as halogens and nitriles, may weaken the π densities of aromatic rings, leading to attenuation of the $\pi-\pi$ interactions with Tyr652s or Phe656. Alternatively, addition of a bulky group such as an ethoxy group may interfere with the contact between the two aromatic rings.

Fexofenadine, a carboxyl derivative of terfenadine (see Chart 1), is nearly devoid of hERG inhibitory activity (IC_{50} = 65 μM).[22] In our preliminary docking study, fexofenadine adopted a binding mode similar to that of terfenadine, where the carboxyl group was not directly involved in the interaction (data not shown). Stansfeld et al. also reported a binding conformation of fexofenadine similar to that of terfenadine.[23] The lack of inhibitory action, therefore, cannot be explained by the binding mode, and further studies are necessary.

Conclusion

In this study, a synergic approach was utilized to elucidate the drug binding modes of the hERG channel. A patch-clamp experiment using tandem dimers was performed, and the drug actions on a set of mutant channels were categorized from the patterns of the inhibition curves, allowing the number and relative position of the residues involved in drug binding to be identified. This information guided the building of a homology model and the elucidation of drugs docking with the hERG channel, leading to realistic models of hERG channel drug binding. The present binding mode demonstrated, in contrast to earlier reports,[5,9] that the cation$-\pi$ interaction may not be the main interaction in all cases, and π-related noncanonical interactions, such as $\pi-\pi$ and CH$-\pi$ interactions, could play a key role. For the cationic moiety of these blockers, it is plausible that the positive charge is driven to the binding site under the weak electric field in the pore region of the hERG potassium channel, especially at depolarized potentials. The interplay between mutational experiments and computational studies, or the synergic approach, enabled us to visualize three-dimensional images of the drug binding, which gave rise to inspiring insights into the modification of any given structure to mitigate hERG binding.

Experimental Section

Construction of Tandem Dimers. The monomeric wild type hERG cDNA was cloned at Takeda Pharmaceutical Company Ltd. and subcloned into the NheI and EcoRI sites in pcDNA3.1(+) plasmid expression vector (Invitrogen, Carlsbad, CA). The hERG mutations were generated by overlap extension polymerase chain reaction (PCR) using PLATINUM Taq DNA Polymerase High Fidelity (Invitrogen, Carlsbad, CA), which was confirmed by sequencing the mutated region and also restriction enzyme analysis. The monomeric mutant harboring S624A, Y652A, or F656A was made by introducing the mutated fragment into the hERG channel gene in the pcDNA3.1(+) vector. The hERG tandem dimers were constructed by linking two monomers that were prepared separately. For the N-terminal side monomer, the wild type hERG channel gene in pcDNA3.1(+) was modified by deleting its stop codon. For the C-terminal side monomer, the hERG channel gene (wild type, harboring Y652A or F656A) was subcloned downstream of the in-frame EcoRI site (note: the original NheI site in front of the first methionine of the channel gene was modified to a unique EcoRI site when subcloned) in the pKF3 vector (Takara Bio, Japan). To generate tandem dimers, the entire channel coding region in the pKF3 vector was digested out with EcoRI and then ligated into the pcDNA3.1(+) vector harboring the stop codon-deleted channel gene. The two monomers were linked by the nucleotide sequence GAATTC.

hERG Expressing Cell Lines. Experiments were performed on human embryonic kidney (HEK-293) cells stably expressing wild type (WT) or mutant hERG. Cells were maintained at 37 °C in minimum Eagle medium (MEM) supplemented with 10% fetal bovine serum, 2 mM L-glutamine, 0.1 mM nonessential amino acids, 1 mM sodium pyruvate, and 0.2 mg/mL Geneticin (Invitrogen Corp., Carlsbad, CA).

Electrophysiology. Whole-cell voltage clamp recordings of hERG currents were made for HEK-293 cells. Borosilicate glass pipettes (Harvard Apparatus, Kent, U.K.) were pulled and fire-polished to get final resistances of 2−3.5 MΩ. The pipet solution contained (in mM) KCl 130, NaCl 7, $MgCl_2$ 1, ATP-2Na 5, HEPES

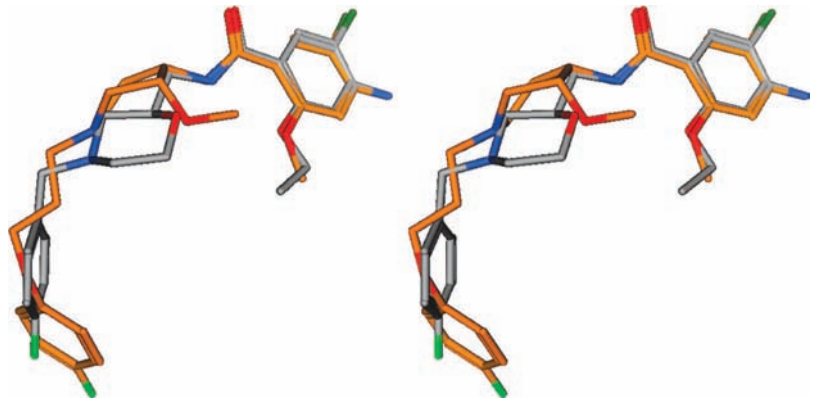

Figure 7. Superposition of mosapride on the binding conformation of cisapride to the hERG channel. Hydrogen atoms are omitted for clarification. Carbon atoms are colored gray for mosapride and colored brown for cisapride. Heavy atoms of both drugs are represented as follows: red, oxygen; blue, nitrogen; green, chlorine; light-green, fluorine.

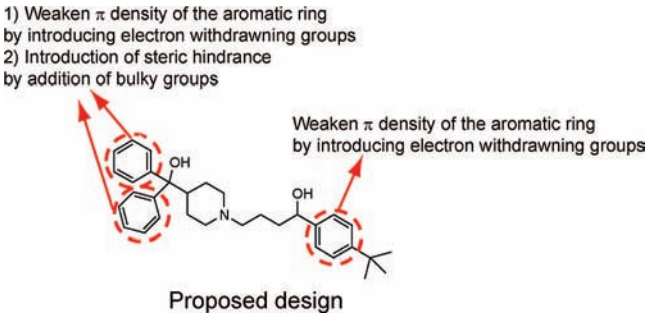

Figure 8. Proposed design for terfenadine to eliminate hERG liability.

5, EGTA 5, pH 7.2. Series resistances were less than 6 MΩ and were compensated by 60−85%. Cells were perfused with Tyrode's solution containing (in mM) NaCl 137, KCl 4, $MgCl_2$ 1, $CaCl_2$ 1.8, glucose 11, HEPES 10, pH 7.4. Whole-cell currents were recorded using an Axopatch 200B amplifier and Clampex software (Molecular Devices Corp., Sunnyvale, CA). Membrane currents were low-pass-filtered at 1 kHz and sampled at 2.5 kHz with a Digidata 1320 data acquisition system (Molecular Devices Corp.).

The membrane potential was held at −75 mV, and depolarization pulses set to 10 mV for 0.5 s were applied. Tail currents were measured at −40 mV. For the recordings of cells expressing the F656A mutant, the hERG current was elicited by a voltage pulse to 0 mV (5 s) from a holding potential of −80 mV. Tail currents were measured upon repolarization to −120 mV (0.5 s). The protocol was repeated every 10 s (15 s for the F656A mutant), allowing complete recovery of the current between test pulses. Experiments were performed at room temperature. Current amplitudes were measured after reaching the steady-state level of drug blockade at each concentration. Normalized currents ($I_{drug}/I_{control}$) were calculated from the peak amplitudes of the tail current before and after the drug applications.

Cisapride (Accurate Chemicals, NY), terfenadine (MP Biochemicals, Eschwege, Germany), and *N*-[4-[[1-[2-(6-methyl-2-pyridinyl)-ethyl]-4-piperidinyl]carbonyl]phenyl] methanesulfonamide dihydrochloride (E-4031, Wako, Japan) were prepared as 10 mM stock solutions in DMSO (dimethyl sulfoxide) and stored at −20 °C. On the day of experiments, the stock solutions were diluted to the desired concentrations with bath solution.

Data Analysis. $I_{drug}/I_{control}$ as a function of drug concentrations was plotted, and the data were fitted to a function. Experimental data were analyzed with Origin software (OriginLab Corp., Northampton, MA). Data are presented as the mean ± SEM.

Docking Studies. The structures of the S5 (outer), pore, and S6 (inner) helices of hERG transmembrane domain were constructed by homology modeling using the known crystal structures in closed state (KcsA, PDB code 1BL8) and open state (MthK, PDB code 1LNQ; KvAP, PDB code 1ORQ) as templates. The template crystal structure was obtained from the RCSB Protein Data Bank[24] as a homotetramer. Sequence alignments were performed by ClustalW 1.6[25] and modified in light of the three-dimensional structures of the templates (Figure 4). Homology modeling was performed by SCWRL 2.9[26] with these alignments. The extracellular loop region was omitted from the models. To build a model that can explain the experimental results, the structures within 7 Å of Ser624 residues in the selectivity filter of the MthK derived model were relaxed using molecular mechanics, where the Amber99 force field was used. Against this model, 40 drug binding poses were generated for each drug molecule, using Gold 2.1.2,[27] with two scoring functions (GoldScore and ChemScore) and default parameters setting. Binding poses satisfying the results from electrophysiological experiments were selected by manual inspection. Energy minimization, docking studies, superposition, and generation of figures were performed using Molecular Operating Environment (MOE).[20]

Acknowledgment. The authors gratefully acknowledge Drs. Kaneyoshi Kato and Hiroyuki Kimura for their suggestions and encouragement and Drs. Toshihiko Myokai and Masayuki Iwamoto for discussions. The authors thank Dr. David Cork for critical reading of the manuscript.

Supporting Information Available: Four pdb files. This material is available free of charge via the Internet at http://pubs.acs.org.

References

(1) Curran, M. E; Splawski, I.; Timothy, K. W.; Vincent, G. M.; Green, E. D.; Keating, M. T. A molecular basis for cardiac arrhythmia: HERG mutations cause long QT syndrome. *Cell* **1995**, *80*, 795–803.

(2) Sanguinetti, M. C.; Jiang, C.; Curran, M. E.; Keating, M. T. A mechanistic link between an inherited and an acquired cardiac arrhythmia: HERG encodes the IKr potassium channel. *Cell* **1995**, *81*, 299–307.

(3) Many articles were reported. A few examples of them are the following: (a) Luo, T.; Luo, A.; Liu, M.; Liu, X. Inhibition of the HERG channel by droperidol depends on channel gating and involves the S6 residue F656. *Anesth. Analg.* **2008**, *106*, 1161–1170. (b) Milnes, J. T.; Witchel, H. J.; Leaney, J. L.; Leishman, D. J.; Hancox, J. C. hERG K^+ channel blockade by the antipsychotic drug thioridazine: an obligatory role for the S6 helix residue F656. *Biochem. Biophys. Res. Commun.* **2006**, *351*, 273–280. (c) Su, Z.; Chen, J.; Martin, R. L.; McDermott, J. S.; Cox, B. F.; Gopalakrishnan, M.; Gintant, G. A. Block of hERG channel by ziprasidone: biophysical properties and molecular determinants. *Biochem. Pharmacol.* **2006**, *71*, 278–286. (d) Witchel, H. J.; Dempsey, C. E.; Sessions, R. B.; Perry, M.; Milnes, J. T.; Hancox, J. C.; Mitcheson, J. S. The low-potency, voltage-dependent HERG blocker propafenone—molecular determinants and drug trapping. *Mol. Pharmacol.* **2004**, *66*, 1201–1212. (e) Scholz, E. P.; Zitron, E.; Kiesecker, C.; Lueck, S.; Kathöfer, S.; Thomas, D.; Weretka, S.; Peth, S.; Kreye, V. A.; Schoels, W.; Katus, H. A.; Kiehn, J.; Karle, C. A. Drug binding to aromatic residues in the HERG channel pore cavity as

possible explanation for acquired long QT syndrome by antiparkinsonian drug budipine. *Naunyn-Schmiedeberg's Arch. Pharmacol.* **2003**, *368*, 404–414. (f) Kamiya, K.; Mitcheson, J. S.; Yasui, K.; Kodama, I.; Sanguinetti, M. C. Open channel block of HERG K^+ channels by vesnarinone. *Mol. Pharmacol.* **2001**, *60*, 244–253.

(4) Many articles were reported. A few examples of them are the following: (a) Ishii, K.; Kondo, K.; Takahashi, M.; Kimura, M.; Endoh, M. An amino acid residue whose change by mutation affects drug binding to the HERG channel. *FEBS Lett.* **2001**, *506*, 191–195. (b) Perry, M.; de Groot, M. J.; Helliwell, R.; Leishman, D.; Tristani-Firouzi, M.; Sanguinetti, M. C.; Mitcheson, J. Structural determinants of HERG channel block by clofilium and ibutilide. *Mol. Pharmacol.* **2004**, *66*, 240–249.

(5) Sánchez-Chapula, J. A.; Navarro-Polanco, R. A.; Culberson, C.; Chen, J.; Sanguinetti, M. C. Molecular determinants of voltage-dependent human ether-a-go-go related gene (HERG) K^+ channel block. *J. Biol. Chem.* **2002**, *277*, 23587–23595.

(6) Mitcheson, J. S.; Chen, J.; Lin, M.; Culberson, C.; Sanguinetti, M. C. A structural basis for drug-induced long QT syndrome. *Proc. Natl. Acad. Sci. U.S.A.* **2000**, *97*, 12329–12333.

(7) Nowak, M. W.; Zacharias, N. M.; Kulkarni, A. A.; Nicholas, J. B.; Sahba, S. D.; Lally, B. S.; Lesso, H. P. S.; Reyes, J.; Mackey, E. D.; Shiva, N. W.; Bennett, P. B. hERG Mutant Panel for Lead Optimization of Compounds with hERG Liability. Presented at the 229th National Meeting of the American Chemical Society, San Diego, CA, March 13−16, 2005; MEDI517.

(8) Myokai, T.; Ryu, S. H.; Shimizu, H.; Oiki, S. Topological mapping of the asymmetric drug binding to the human ether-à-go-go-related gene product (HERG) potassium channel by use of tandem dimers. *Mol. Pharmacol.* **2008**, *73*, 1643–1651.

(9) Fernandez, D.; Ghanta, A.; Kauffman, G. W.; Sanguinetti, M. C. Physicochemical features of the HERG channel drug binding site. *J. Biol. Chem.* **2004**, *279*, 10120–10127.

(10) Ryu, S. H.; Myokai, T.; Imai, Y. N.; Oiki, S. Mutated HERG Channel-Expressing Cells and Their Applications. Patent disclosed in Japan, 2005-269153 and 2007-075042 (applied on Sep 15, 2005, and disclosed on Mar 29, 2007).

(11) Sanguinetti, M. C.; Jurkiewicz, N. K.; Scott, A.; Siegl, P. K. S. Isoproterenol antagonizes prolongation of refractory period by the class III antiarrhythmic agent E-4031 in guinea pig myocytes. *Circ. Res.* **1991**, *68*, 77–84.

(12) Very recently, Kamiya et al. reported that from ala scanning, Ser624 attenuated the hERG blockade by terfenadine, which is inconsistent with our results. Kamiya, K.; Niwa, R.; Morishima, M.; Honjo, H.; Sanguinetti, M. C. Molecular determinants of HERG channel block by terfenadine and cisapride. *J. Pharmacol. Sci.* **2008**, *108*, 301–307.

(13) Farid, R.; Day, T.; Friesner, R. A.; Pearlstein, R. A. New insights about HERG blockade obtained from protein modeling, potential energy mapping, and docking studies. *Bioorg. Med. Chem.* **2006**, *14*, 3160–3173.

(14) Numaguchi, H.; Mullins, F. M.; Johnson, J. P., Jr.; Johns, D. C.; Po, S. S.; Yang, I. C.; Tomaselli, G. F.; Balser, J. R. Probing the interaction between inactivation gating and Dd-sotalol block of HERG. *Circ. Res.* **2000**, *87*, 1012–1018.

(15) Thomas, D.; Wendt-Nordahl, G.; Röckl, K.; Ficker, E.; Brown, A. M.; Kiehn, J. High-affinity blockade of human ether-a-go-go-related gene human cardiac potassium channels by the novel antiarrhythmic drug BRL-32872. *J. Pharmacol. Exp. Ther.* **2001**, *297*, 753–761.

(16) Ringer, A. L.; Figgs, M. S.; Sinnokrot, M. O.; Sherrill, C. D. Aliphatic C−H/π interactions: Methane−benzene, methane−phenol, and methane−indole complexes. *J. Phys. Chem. A* **2006**, *110*, 10822–10828.

(17) Sinnokrot, M. O.; Sherrill, C. D. High-accuracy quantum mechanical studies of $\pi-\pi$ interactions in benzene dimers. *J. Phys. Chem. A* **2006**, *110*, 10656–10668.

(18) (a) Zhou, M.; Morais-Cabral, J. H.; Mann, S.; MacKinnon, R. Potassium channel receptor site for the inactivation gate and quaternary amine inhibitors. *Nature* **2001**, *411*, 657–661 (PDB code 1J95). (b) Morais-Cabral, J. H.; Zhou, Y.; MacKinnon, R. Energetic optimization of ion conduction rate by the K^+ selectivity filter. *Nature* **2001**, *414*, 37–42 (PDB code 1JVM). (c) Yohannan, S; Hu, Y; Zhou, Y. Crystallographic study of the tetrabutylammonium block to the KcsA K^+ channel. *J. Mol. Biol.* **2007**, *366*, 806–814 (PDB codes 2DWD, 2DWE). (d) Faraldo-Gomez, J. D.; Kutluay, E.; Jogini, V.; Zhao, Y.; Heginbotham, L.; Roux, B. Mechanism of intracellular block of the KcsA K^+ channel by tetrabutylammonium: insights from X-ray crystallography, electrophysiology and replica-exchange molecular dynamics simulations. *J. Mol. Biol.* **2007**, *365*, 649–662 (PDB code 2HJF). (e) Yohannan, S.; Hu, Y.; Zhou, Y. Crystallographic study of the tetrabutylammonium block to the KcsA K^+ channel. *J. Mol. Biol.* **2007**, *366*, 806–814 (PDB codes 2HVJ, 2HVK).

(19) Toga, T.; Kohmura, Y.; Kawatsu, R. The 5-HT(4) agonists cisapride, mosapride, and CJ-033466, a novel potent compound, exhibit different human ether-a-go-go-related gene (hERG)-blocking activities. *J. Pharmacol. Sci.* **2007**, *105*, 207–210.

(20) *MOE (Molecular Operating Environment)*; Chemical Computing Group: Montreal, Quebec, Canada, 2005.

(21) Kamiya, K.; Niwa, R.; Mitcheson, J. S.; Sanguinetti, M. C. Molecular determinants of HERG channel block. *Mol. Pharmacol.* **2006**, *69*, 1709–1716.

(22) Rajamani, S.; Anderson, C. L.; Anson, B. D.; January, C. T. Pharmacological rescue of human K^+ channel long-QT2 mutations: human ether-a-go-go-related gene rescue without block. *Circulation* **2002**, *105*, 2830–2835.

(23) Stansfeld, P. J.; Gedeck, P.; Gosling, M.; Cox, B.; Mitcheson, J. S.; Sutcliffe, M. J. Drug block of the hERG potassium channel: insight from modeling. *Proteins* **2007**, *68*, 568–580.

(24) Berman, H. M.; Westbrook, J.; Feng, Z.; Gilliland, G.; Bhat, T. N.; Weissig, H.; Shindyalov, I. N.; Bourne, P. E. The Protein Data Bank. *Nucleic Acids Res.* **2000**, *28*, 235–242.

(25) Thompson, J. D.; Higgins, D. G.; Gibson, T. J. CLUSTAL W: improving the sensitivity of progressive multiple sequence alignment through sequence weighting, position-specific gap penalties and weight matrix choice. *Nucleic Acids Res.* **1994**, *22*, 4673–4680.

(26) Bower, M. J.; Cohen, F. E.; Dunbrack, R. L., Jr. Prediction of protein side-chain rotamers from a backbone-dependent rotamer library: a new homology modeling tool. *J. Mol. Biol.* **1997**, *267*, 1268–1282.

(27) Jones, G.; Willet, P.; Glen, R. C. Molecular recognition of receptor sites using a genetic algorithm with a description of desolvation. *J. Mol. Biol.* **1995**, *245*, 43–53.

JM801236N